

## Manuscript Details

<b>Manuscript number</b>	STILL_2018_15
<b>Title</b>	A theoretical study of the limit path of the movement of a layer of soil along the plough mouldboard
<b>Article type</b>	Research Paper

### Abstract

There have been studied regularities affecting the magnitude of the dynamic component of the plough resistance for cylindrical mouldboards, and its peculiarities for cylindrical mouldboards depending on the direction of arrival of the soil layer on the ploughshare. The dynamic component of the draught resistance of the plough, which is directly proportional to the square of the ploughing velocity, can be estimated by the value of a dimensionless coefficient, conditionally named the "wrapping angle of the layer". This coefficient can be found for the mouldboard surface if the path of the movement of the mid-point of the section of the soil layer is known. By example of a cylindrical surface of the mouldboard it is shown how the dynamic component of the resistance varies depending on the design parameters of the mouldboard and the direction of arrival of the soil layer onto the ploughshare.

<b>Keywords</b>	layer of soil; mouldboard of the plough; geodesic line
<b>Taxonomy</b>	Tilth, Soil Mechanics, Soil Traction Mechanics, Tillage Equipment, Plough Draught Prediction
<b>Manuscript category</b>	Soil Management
<b>Corresponding Author</b>	Simone Pascuzzi
<b>Corresponding Author's Institution</b>	Department of Agro-Environmental Science
<b>Order of Authors</b>	Volodymyr Bulgakov, Simone Pascuzzi, Valerii Adamchuk, Semjons Ivanovs, Serhiy Pylypaka
<b>Suggested reviewers</b>	Mykola SVIREN, DOMENICO PESSINA, Danilo Monarca, Viktor MELNYK, Michele Raffaelli

## Submission Files Included in this PDF

### File Name [File Type]

Cover\_letter.doc [Cover Letter]

Highlights.docx [Highlights]

manuscript\_10.doc [Manuscript File]

To view all the submission files, including those not included in the PDF, click on the manuscript title on your EVISE Homepage, then click 'Download zip file'.

Dear,

I wish to submit for referring the manuscript:

"A theoretical study of the limit path of the movement of a layer of soil along the plough mouldboard" written by Volodymyr Bulgakov, Simone Pascuzzi, Valerii Adamchuk, Semjons Ivanovs, Serhiy Pylypaka

I think that the topic covered in the paper can be interesting for your Journal and I am ready to follow your suggestions in order to improve the work.

Thank you!

Kindly acknowledge the reception of this mail.

Best regards  
Simone Pascuzzi

Prof. Simone Pascuzzi  
Department of Agricultural and Environmental Science  
University of Bari Aldo Moro  
Via Amendola 165/A  
70126 Bari Italy  
e-mail: [simone.pascuzzi@uniba.it](mailto:simone.pascuzzi@uniba.it)  
Tel. - Fax +39 0805442214  
Mobil +39 320 7980619

## **Highlights**

- Motion of a soil layer along mouldboards and dynamic component of draught resistance.
- Dynamic component of plough draught resistance and "wrapping angle of layer" factor.
- Mouldboard design and arrival angle of soil layer onto ploughshare affect resistance.
- The proposed approach considers only the geometry of the surface of mouldboards.

1 **A theoretical study of the limit path of the movement of a layer of soil along the plough**  
2 **mouldboard**

3

4 **Volodymyr Bulgakov<sup>a</sup>, Simone Pascuzzi<sup>b,\*</sup>, Valerii Adamchuk<sup>c</sup>, Semjons Ivanovs<sup>d</sup>, Serhiy Pylypaka<sup>a</sup>**

5

6 <sup>a</sup>National University of Life and Environmental Sciences of Ukraine, *Heroyiv Oborony 15, Kyiv,*  
7 *03041, – Ukraine*

8

9 <sup>b</sup>Department of Agricultural and Environmental Science, University of Bari Aldo Moro, *Via*  
10 *Amendola 165/A – 70126 Bari – Italy*

11

12 <sup>c</sup>National Scientific Centre “Institute for Agricultural Engineering and Electrification”, *Vokzalna 1,*  
13 *Glevaha, 1108631, Ukraine*

14

15 <sup>d</sup>Latvia University of Agriculture, *Instituta 1, Ulbroka, LV-2130 – Latvia*

16

17 \*Corresponding Author:

18 Simone Pascuzzi

19 Via Amendola, 165/A – 70125 Bari, ITALY.

20 Tel. & fax: 0039 0805442214

21 email address: [simone.pascuzzi@uniba.it](mailto:simone.pascuzzi@uniba.it)

22

23

25 **Abstract**

26 There have been studied regularities affecting the magnitude of the dynamic component of the  
27 plough resistance for cylindrical mouldboards, and its peculiarities for cylindroical mouldboards  
28 depending on the direction of arrival of the soil layer on the ploughshare. The dynamic component  
29 of the draught resistance of the plough, which is directly proportional to the square of the ploughing  
30 velocity, can be estimated by the value of a dimensionless coefficient, conditionally named the  
31 "wrapping angle of the layer". This coefficient can be found for the mouldboard surface if the path  
32 of the movement of the mid-point of the section of the soil layer is known. By example of a  
33 cylindroical surface of the mouldboard it is shown how the dynamic component of the resistance  
34 varies depending on the design parameters of the mouldboard and the direction of arrival of the soil  
35 layer onto the ploughshare.

36

37 **Keywords:** layer of soil, mouldboard of the plough, path of the movement, geodesic line.

38

## 40 **1. Introduction**

41 Soil tillage requires great amount of energy in agricultural production and in last decades a topic of  
42 interest of many researchers has been the evaluation of tillage draught (Karmakar and Kushwaha,  
43 2006; Tong and Moayad, 2006; Bentaher et al., 2008; Shmulevich, 2010). Taking into account that  
44 the tillage forces are mainly a function of soil mechanical properties, working parameters of the tool  
45 (e.g. depth and speed) and tool geometry, simulation of soil-tool interaction for farming operations  
46 has also been analysed for the design and optimization of tillage implements (Zhang et al., 2018;  
47 Abo-Elnor, et al. 2004; Zhu et al., 2017; Bentaher, et al., 2013; Chi and Kushwaha, 1990).

48 In the well-known rational formula of the draught resistance force of the plough, obtained by  
49 V.Goryachkin, there are three components, one of which is directly proportional to the square of the  
50 velocity of relative movement of the layer along the mouldboard. It is the so-called dynamic  
51 component (Goryachkin, 1998). These components are in complex dependence on the properties of  
52 the soil, the speed of ploughing, the shape of the mouldboard surface. The author of this formula  
53 himself noted: "... in the future, in a more detailed study, each of the three terms of the formula may  
54 have to be developed and replaced by more complex functions." Therefore, the search for new  
55 dependencies of these components of the draught resistance of the plough upon its design  
56 parameters is an actual scientific task.

57 L.Gyachev considered in detail the forces that arise during the interaction of the soil layer with the  
58 mouldboard, and compiled a differential equation for the path of the movement of the mid-point of  
59 the soil layer along the mouldboard (Gyachev, 1981). In addition, he took into account the  
60 dimensions and specific gravity of the soil layer, its elasticity, the ploughing velocity, and linked  
61 these parameters with the normal and geodesic curvature, and the length of the path. From the  
62 compiled differential equation he obtained a result according to which, when the rigidity of the soil  
63 layer and velocity of its movement along the mouldboard increases, the geodesic curvature of the  
64 path approaches zero, i.e. the soil layer tends to move along the geodesic line of the surface, which  
65 is the upper limit path. Thus the search for the ultimate path of the layer movement is reduced to

66 finding the geodesic line of the mouldboard surface, which, in its turn, makes it possible to consider  
67 interaction of the layer with the mouldboard.

68 A.Vilde, who developed the theory by V.Goryachkin, investigated the draught resistance of helical  
69 mouldboard surfaces of the plough under the conditions of Latvia (Vilde, 2004, Rucins et al., 2007,  
70 Vilde, 2008). Although a number of contemporary researchers have continued research in the  
71 plough surfaces in order to improve the quality of soil cultivation in particular soil and climatic  
72 zones, and to reduce energy requirement, these tasks still remain topical. By means of the created  
73 test-bench, profilograms (shape lines) were obtained for the share-mouldboard surfaces of some  
74 bodies mainly used on the farms of Latvia, as well as their parameters and suitability for the Latvian  
75 conditions were determined (Vilde, 2012).

76 It is well known that geodesic lines on a surface are the shortest paths between two points on the  
77 surface (Volkov, 2002). Just as it is possible to draw a bundle of straight lines in all directions, it is  
78 possible to draw a bundle of geodesic lines from a point on the surface, among which there can be  
79 straight lines (forming surfaces if the surface is linear) and curves (planar and spatial). P.Vasilenko  
80 pointed out that in the case of the movement of a material point by inertia, in order to determine the  
81 path of this movement, one can use the solution of the differential equation of the geodesic line  
82 instead of solving the differential equation of the movement of a point (Vasilenko, 1980). Geodesic  
83 lines on the surface are described by second-order differential equations, for which numerical  
84 methods must be applied. Modern means of the computer technology provide a possibility not only  
85 to find them but also to visualise (Bulgakov, 2010).

86 However, it is possible to do the opposite - to set the desired limit path of the movement of the soil  
87 layer and, with its help, to find the surface itself. Designing the plough mouldboard from unfolding  
88 surfaces along a pre-set limit path of the layer movement without a force interaction is discussed in  
89 (Bulgakov, 2011).

90 The aim of this work was a theoretical study of the limit path of the movement of a soil layer along  
91 the linear surfaces of the mouldboards and its impact upon the dynamic component of the draught  
92 resistance of the plough.

93

## 94 **2. Materials and Methods**

95 In the analytical study, there were used methods of agricultural mechanics, higher mathematics and  
96 differential geometry, as well as programming and numerical calculations on the PC were used.

97 If the soil is hard, coherent, intertwined with plant roots, then its movement along the mouldboard  
98 differs from the movement of a loose (incoherent) soil. Let us consider interaction of such a soil  
99 with a part of a cylindrical surface, which we refer to a three-dimensional coordinate system  $xyz$   
100 (Figure 1). In this case, the lower generatrix of this surface makes angle  $\gamma$  with axis  $y$ . The  
101 tangent plane to the cylinder along the lower generatrix is inclined to the horizontal plane at angle  
102  $\varepsilon$ . In the way considered a part of this cylindrical surface can be regarded as a plough mouldboard.  
103 Then the path of the movement of the elastic layer of the soil along the plough mouldboard can be  
104 simulated with some approximation in the form of a movement of a narrow, flexible, elastic band if  
105 it is somehow moved along the mouldboard in a pre-set direction at angle  $\gamma$ . The direction of  
106 movement of this band is indicated by an arrow (Fig. 1 a).

107 If the band adheres to the surface, then its position will determine the geodesic line. The actual path  
108 of the soil layer will differ from the one described in the case with a flexible elastic band because,  
109 under the action of its weight, it will deflect downwards along the mouldboard.

110 Let us consider theoretical preconditions for the formation of a path by example of a cylindrical  
111 surface since the differential equations for finding geodesic lines on it are greatly simplified, and the  
112 geodesic lines of such a surface themselves are easy to perceive – they all intersect the rectilinear  
113 generatrices at a constant angle  $\gamma$ , and after unfolding they turn into straight lines.

114 Next we will simulate the movement of the soil layer, distinguishing in it an infinitely small  
115 element (elementary parallelepiped) having geometric dimensions  $a$ ,  $b$  and  $ds$  (Fig. 1 b).



116 In a general case of movement this infinitesimal element is taken as a material particle.  
117 We suppose that this material particle is moving along the spatial curve with acceleration, one  
118 component of which being directed along tangent  $\bar{\tau}$ , and the second – in the direction of the main  
119 normal  $\bar{n}$  of the curve at the point where this particle is located. If the material particle is moving  
120 at a constant velocity along the curve (and we accept just this case since velocity  $V$  of the  
121 movement of the soil layer along the mouldboard is equal to the velocity of the plough movement  
122 aggregated with the tractor, and it is constant by its magnitude), then the first component will be  
123 zero, and the value of the second component is determined from expression  $V^2k$ , where  $k$  is the  
124 curvature of the path at the point of location of the material particle. If the curve (i.e. the path of the  
125 movement) is located on the surface, then the material particle will interact with it creating pressure  
126 with a certain force  $F$ . The pressure force, like the surface reaction, is always directed along  
127 normal  $\bar{n}$  towards the surface. On the whole, this force of pressure is created by components of the  
128 weight of the material particle, the centrifugal force, the force that bends the layer of the soil in case  
129 it is sufficiently elastic, and other less significant forces. Besides, if the weight of a material particle  
130 does not depend on the curvature of the path, then the curvature of the path has a significant impact  
131 upon the last two components of the indicated pressure force.

132

133 Let us consider in greater detail this material particle moving along the inner surface of a cylinder  
134 (Fig. 2). Let this particle (the element of the soil layer) be at point  $A$  of the path of movement.  
135 Through point  $A$  we will draw vectors of a natural trihedron of the path - the tangent line  $\bar{\tau}$  and  
136 the principal normal  $\bar{n}$ . The curvature vector  $k$  will be directed along the principal normal  $\bar{n}$  of  
137 the path. The centrifugal force  $\bar{F}_c$  acting upon the material particle and defined by such an  
138 expression:

139 
$$F_c = mV^2k, \quad (1)$$

140 is directed in the opposite direction.

141 At point  $A$  of the path we will draw plane  $\mu$ , tangent to the cylinder. The perpendicular, drawn to  
142 this plane  $\mu$  at point  $A$  is a normal  $\bar{N}$  to the surface of the cylinder.

143 The direction of the centrifugal force  $\bar{F}_c$  does not coincide with the direction of the normal  $\bar{N}$  to  
144 the surface; therefore the vector of its action must be decomposed into components along the  
145 normal  $\bar{n}$  to the surface and onto the tangent plane  $\mu$ . This is equivalent to the decomposition of  
146 curvature  $k$  along the same directions, component  $k_n$  on the normal  $\bar{N}$  to the surface being  
147 named a normal curvature, and component  $k_g$  on the tangent plane  $\mu$  to the surface – a geodesic  
148 curvature.

149 Angle  $\varepsilon$  between the normal  $\bar{N}$  to the surface and the principal normal  $\bar{n}$  of the path through  
150 which decomposition is carried out is determined by the methods of differential geometry, and it  
151 depends on the shape of the curve on the surface. In a general case it is variable and depends on the  
152 location of the point on the curve, as well as curvature  $k$ , i.e.:

$$153 \quad \varepsilon = \varepsilon(s), \quad (2)$$

154 and

$$155 \quad k = k(s), \quad (3)$$

156 where  $s$  – arc length of the arc of the curve, m.

157

158 For the geodesic line, angle  $\varepsilon$  is zero at all points, i.e., the principal normal  $\bar{n}$  of the curve  
159 coincides with the normal  $\bar{N}$  to the surface.

160 Let us suppose further that elasticity of the soil layer is sufficiently small, i.e., it practically does not  
161 exert resistance to the bend of the layer. Then two forces act upon the element of the soil layer of  
162 the size  $a \times b \times ds$  (Fig. 1 b), which we will further consider as elementary: the elementary force of  
163 weight, equal to:

$$164 \quad dP = (a \times b \times ds) \eta \cdot g = a \cdot b \cdot \eta \cdot g \cdot ds, \quad (4)$$

165 where  $\eta$  – the soil density,  $\text{kg}\cdot\text{cm}^{-3}$ ;  $g$  – acceleration of gravity,  $\text{m}\cdot\text{s}^{-2}$ ;

166

167 and the elementary centrifugal force, which will be equal to:

$$168 \quad dF_c = mV^2k = a \cdot b \cdot \eta \cdot V^2 \cdot k \cdot ds . \quad (5)$$

169 Both these forces must be decomposed along the directions, as shown in Fig. 2. The component of  
170 the elementary centrifugal force  $dF_c$  projected on the normal  $\bar{N}$  to the surface, creates pressure of  
171 the soil layer element on the mouldboard. Its value is determined from this expression:

$$172 \quad dF_{cn} = a \cdot b \cdot \eta \cdot V^2 \cdot k_n \cdot ds . \quad (6)$$

173 This force is balanced by the reaction of the cylinder surface.

174 The second component, equal to:

$$175 \quad dF_{cg} = a \cdot b \cdot \eta \cdot V^2 \cdot k_g \cdot ds , \quad (7)$$

176 which is projected onto the tangent plane, is balanced by the component of the weight force of the  
177 layer element (in case the force of weight is projected onto the tangent plane):

$$178 \quad mg_c = a \cdot b \cdot \eta \cdot g \cdot ds_c , \quad (8)$$

179 where  $ds_c$  – the projection of the length of the elementary parallelepiped onto the tangent plane  $\mu$ .

180

181 The soil layer, as a rule, does not exert great resistance to bending, and the component of the part of  
182 the weight  $mg_c$  deflects it in the tangent plane from the rectilinear direction. Nevertheless, when  
183 increasing the ploughing velocity  $V$ , the component of the centrifugal force  $dF_{cg}$  increases directly  
184 in proportion to the square of velocity, i.e., with a slight increase in velocity, the component of the  
185 centrifugal force  $dF_{cg}$  increases very significantly.

186 Since the value of the component force of weight  $mg_c$ , which balances it, does not depend on  
187 velocity  $V$ , the increasing component of the centrifugal force  $dF_{cg}$  tries to straighten the path of  
188 the movement of the soil layer element, bringing it closer to the geodesic line. With infinite

189 increasing in velocity  $V$ , the geodesic line will be the path of the movement of the soil layer.  
190 Consequently, the geodesic line can be considered as the limit path of the movement of the soil  
191 layer, which can be real for it at a high ploughing velocity or an absolutely elastic soil layer.

192 Let us further consider the action of forces when the soil layer is elastic and exerts a certain  
193 resistance to its bending. In this case the soil layer bends in two directions: in the tangent and the  
194 normal planes of the path. However, in these planes its resistance to bending will be different and it  
195 will depend on the hardness of the soil layer. The rigidity of the layer depends on the geometric  
196 dimensions of the section of the soil layer and is determined, in its turn, by the product  $E$  of the  
197 elastic modulus of the soil by the inertia moment  $I$  of the section of the soil layer. For normal and  
198 tangential planes, the rigidity ( $EI$ ) of the soil layer will accordingly have the following values:

199 
$$EI_n = \frac{Eab^3}{12}, \quad (9)$$

200 and

201 
$$EI_g = \frac{Ea^3b}{12}. \quad (10)$$

202 Since  $a > b$ , then rigidity  $EI_g$  and, accordingly, the resistance to the bend of the soil layer will be  
203 greater in the tangent plane than in the normal plane.

204 So another factor that approximates the path of the movement to the geodesic line of the  
205 mouldboard is increase in the width of the strip in comparison with its height, i.e., the depth of  
206 ploughing.

207 In order to find the forces necessary for bending the soil layer in both planes, we will use the well-  
208 known provisions of the theory of material resistance according to which curvature  $k$  of the elastic  
209 axis of the rod is directly proportional to the applied moment  $M$  and inversely proportional to the  
210 rigidity of the rod, i.e.:

211 
$$k = \frac{M}{E \cdot I}. \quad (11)$$

212 After finding moment  $M$  and its differentiating along the length of the elastic axis (in this case  
 213 along the length of path  $S$ ), we will obtain a force that bends the layer of the soil. Another  
 214 differentiation will give a distributed force per unit of the length of the path.

215 Thus the force for bending  $F_b$  of the layer along its length within the limits of the mouldboard is  
 216 determined from such expressions:

217 – in a normal plane:  $F_{bn} = \frac{dM_n}{ds} = E \frac{ab^3}{12} \frac{dk_n}{ds}$ , (12)

218 – in a tangent plane:  $F_{bg} = \frac{dM_g}{ds} = E \frac{a^3b}{12} \frac{dk_g}{ds}$ . (13)

219 The soil layer creates pressure upon the mouldboard with a force determined by expression (12),  
 220 causing a friction force  $fF_{bn}$ , where  $f$  is the coefficient of friction of the soil layer along the  
 221 mouldboard. However, it also depends on the elasticity of the soil layer and may be absent in the  
 222 case when the soil layer does not exert resistance to bending. At the same time, the normal  
 223 component of the centrifugal force is always present and does not depend on the properties of the  
 224 soil (bearing in mind that its density is constant). Since the elementary force with which the element  
 225 of the soil layer presses upon the mouldboard is determined from expression (6), then it is necessary  
 226 to integrate this expression along the length of arc  $S$  of the path. Assuming that the dimensions of  
 227 the section of the soil layer are constant, the ploughing velocity and the soil density are constant,  
 228 force  $F_{cn}$  will be determined from such an expression:

229 
$$F_{cn} = a \cdot b \cdot \eta \cdot V^2 \int k_n ds .$$
 (14)

230 Consequently, the force of pressure, caused by the action of the centrifugal force, which is always  
 231 present in the case of a curvilinear path, can be reduced by decreasing the integral entering into  
 232 expression (14). Yet this characteristic curve on the surface is purely geometric and does not depend  
 233 on the properties of the soil. It will be determined if the path of the soil layer movement along the  
 234 mouldboard is determined. However, if we assume that the path of the soil layer approaches the  
 235 geodesic line or moves along it, then the problem of finding this integral becomes quite definite.

236 In this case angle  $\varepsilon$  (Fig. 2 a) becomes equal to zero and  $k_n = k$ , i.e. decomposition of the  
 237 curvature vector does not occur, and the entire centrifugal force acts along the normal to the surface  
 238 of the mouldboard. This integral has a geometric sense, which follows from the definition of the  
 239 curvature  $k$  of the curve. Since:

$$240 \quad k = \frac{d\theta}{ds}, \quad (15)$$

241 then:

$$242 \quad \theta = \int k ds, \quad (16)$$

243 where  $\theta$  – an angle at which the tangent to the curve turns as it moves along it from the initial to  
 244 the final value of the arc.

245 Professor L.Gyachev named it the "wrapping angle of the mouldboard". In this case this angle is  
 246 measured in radians but can be translated into degrees. It will be possible to show this angle on the  
 247 mouldboard of the plough, taking into account certain geometric peculiarities. Thus it can be seen  
 248 on the cylindrical surface in case the angle of entry of the layer is  $= 90^\circ$ .

249 As already mentioned, the geodesic lines on the cylindrical surfaces intersect the rectilinear  
 250 generatrices at a constant angle  $\gamma$  and, on its unfolding, they turn into straight lines. If this angle is  
 251 straight, then the geodesic line is an orthogonal section of the cylinder, i.e., it is flat. In the case  
 252 when  $\gamma = 0$ , the geodesic line is the rectilinear generatrix of the surface. At all the other values of  
 253 angle  $\gamma$ , the geodesic lines are the spatial curves. If they are all projected onto a plane  
 254 perpendicular to the generatrices of the cylinder, then their projection will be a flat curve – an  
 255 orthogonal section of the cylinder. There is a relationship between the curvature  $k$  of the curve and  
 256 the curvature  $k_s$  of its projection (i.e., the cross section of the cylinder), as well as between the  
 257 lengths of their arcs  $s$  and  $s_s$ , which are determined by such well-known expressions:

$$258 \quad k = k_s \cdot \sin^2 \gamma, \quad (17)$$

259 and

$$ds = \frac{ds_s}{\sin \gamma} . \quad (18)$$

Using expressions (17) and (18) and substituting them into expression (16), we can write the dependence of angle  $\theta$  in this way:

$$\theta = \int k ds = \sin \gamma \int k_s ds_s . \quad (19)$$

When analysing dependence (19), one can draw an important conclusion that the greatest value of angle  $\theta$  will be at  $\gamma = 90^\circ$ , i.e., for a flat curve of an orthogonal section of the cylinder. For other values of angle  $\gamma$ , it decreases in direct proportion to its sine.

For better understanding of the essence of this angle we will discuss a concrete example of geodesic lines on a cylindrical surface. Let the orthogonal section of the cylinder be an arc of the parabola, located in a vertical plane and having parametric equations, which ultimately determine its appearance:

$$x = -v , \quad (20)$$

$$z = av^2 ,$$

where  $a$  – a constant value, i.e., the parameter of the parabola shape parameter;  $v$  – an independent variable.

Such an approach previously found sufficiently wide application in designing the plough mouldboards when a parabola is adopted as the curve for the cross section of the cylinder, which was set by several parameters: the starting point on the blade of the ploughshare, drawn through its tangent, the angle of inclination of the rear side of the ploughshare to the bottom of the furrow, and the end point with the tangent drawn to it. Despite the fact that the circumference of the cylinder may be a circle (or any other curve), the cross section of the cylinder in the form of a parabola, however, has undoubted advantages connected with the control of the shape of the curve by changing the angles of inclination of the tangents at the initial and final points, and changing

285 distances between the points. In addition, it was more convenient to draw, using graphical methods  
 286 without the application of equations. In any case, the presence of a curve of the cross section of the  
 287 mouldboard is necessary as a guiding curve of the surface.

288 The parametric equations of the cylinder can be written as follows:

$$\begin{aligned}
 289 \quad & X = -v, \\
 290 \quad & Y = -u, \\
 291 \quad & Z = av^2,
 \end{aligned} \tag{21}$$

292 where  $u$  – the second independent variable (in this case it is the length of the rectilinear  
 293 generatrix).

294 The cross-section of a surface with height  $h$  and a length of generatrices, equal to five linear units,  
 295 is shown in Fig. 3 a. In order to build a line on the surface, we have to join together two  
 296 independent variables  $u$  (the length of a straight-line generatrix) and  $v$  with a certain dependency.  
 297 For the curve intersecting all generatrices at a constant angle  $\gamma$ , i.e., the geodesic curve, this  
 298 dependency has the form:

$$299 \quad u = \operatorname{ctg} \gamma \int \sqrt{x'^2 + z'^2} dv = \operatorname{ctg} \gamma \int \sqrt{1 + 4a^2 v^2} dv = \frac{2av\sqrt{1 + 4a^2 v^2} + \operatorname{Arcsinh}(2av)}{4a \cdot \tan \gamma}, \tag{22}$$

300 where  $\operatorname{Arcsinh}$  – the hyperbolic arcsine.

301

302 Consequently, on the cylindrical surface (21) the parametric equations of the geodesic line acquire  
 303 the following form:

$$\begin{aligned}
 & x_g = -v, \\
 304 \quad & y_g = -\frac{2a \cdot v\sqrt{1 + 4a^2 v^2} + \operatorname{Arcsinh}(2av)}{4a \cdot \operatorname{tg} \gamma}, \\
 & z_g = av^2.
 \end{aligned} \tag{23}$$

305

306 In Fig. 3 a, on the cylindrical surface (21) geodesic lines are constructed according to equations (23)  
 307 for different angles of arrival of the layer onto the surface, including angle  $\gamma = 42^\circ$  accepted for the



308 ploughs. Let us find the wrapping angle  $\theta$  of the layer by the section of the surface of the  
 309 mouldboard for each of these lines. We find curvature  $k$  and the differential of arc  $ds$  through the  
 310 first and second derivatives according to the known formulas (we present the final results of  
 311 differentiation):

$$312 \quad k = \frac{\sqrt{\begin{vmatrix} y'_g & z'_g \\ y''_g & z''_g \end{vmatrix}^2 + \begin{vmatrix} z'_g & x'_g \\ z''_g & x''_g \end{vmatrix}^2 + \begin{vmatrix} x'_g & y'_g \\ x''_g & y''_g \end{vmatrix}^2}}{(x'_g{}^2 + y'_g{}^2 + z'_g{}^2)^{3/2}} = \frac{2a \sin^2 \gamma}{(1 + 4a^2 v^2)^{3/2}}. \quad (24)$$

$$313 \quad ds = \sqrt{x'_g{}^2 + y'_g{}^2 + z'_g{}^2} dv = \frac{\sqrt{1 + 4a^2 v^2}}{\sin \gamma} dv. \quad (25)$$

314 Consequently, the wrapping angle  $\theta$  of the layer will be equal to:

$$315 \quad \theta = \int k ds = 2a \sin \gamma \int \frac{dv}{1 + 4a^2 v^2} = \sin \gamma \operatorname{Arctg}(2av). \quad (26)$$

316 By formula (26) one can find angle  $\theta$  for any of the geodesic lines shown in Fig. 3 a. Since for all  
 317 of them changing parameter  $v$  occurs within the same boundaries (from  $v_1$  the moment when the  
 318 layer enters the lower generatrix to  $v_2$  when it leaves the upper generatrix), the values of angle  $\theta$   
 319 will differ with each other, depending on  $\sin \gamma$ , i.e., we get a result, found earlier. Hence it follows  
 320 that, when the layer is raised to the same height  $h$  (Fig. 3), the greatest force of pressure and,  
 321 accordingly, the draught resistance will be at  $\gamma = 90^\circ$ , i.e., when the layer is lifted by the shortest  
 322 path perpendicular to the generatrices. At  $\gamma = 30^\circ$ , the draught resistance is reduced two times,  
 323 although the path of the layer increases. This is explained by the fact that the curvature of the path  
 324 decreases more intensely. Nevertheless, if we follow this way by reducing the draught resistance,  
 325 we have to increase the length of the mouldboard significantly. Obviously, the value of angle  $\theta$   
 326 does not depend on the point of arrival of the layer onto the lower generatrix at a preset angle  $\gamma$ .

327 Now let us discuss the physical essence of angle  $\theta$ . It can be best seen (and at the same time it  
 328 corresponds to its name) at  $\gamma = 90^\circ$ . In this case the tangent to the path of its movement from the

329 lower to the upper point turns by angle  $\varphi$  (Fig. 3 b). Accordingly, the normal to the surface turns  
330 by the same angle, i.e., this is the angle between the lower and upper normals when the layer is  
331 elevated to a particular height  $h$ . For this case  $\theta = \varphi$ . For other paths at  $\gamma \neq 90^\circ$  angle  $\theta$  is  
332 determined by multiplying angle  $\varphi$  by  $\sin \gamma$ , i.e., it will be smaller despite the same height  $h$  of  
333 elevation. This can be explained by the fact that angle  $\theta$  arises by turning not the normal in relation  
334 to the surface along the path but the tangent to the path, and only at  $\gamma = 90^\circ$  these angles are equal.

335 If for the cylindrical surface the relationships of the formation of angle  $\theta$  have been clarified and  
336 described by relatively simple dependences, for more complex (non-unfolding) surfaces its finding  
337 becomes more complicated. Let us consider the peculiarities of the formation of angle  $\theta$  for  
338 cultural cylindrical mouldboards. Cylindroidal surfaces are linear non-unfolding ones, and, in order  
339 to find the geodesic lines on them, it is necessary to solve the second-order differential equations  
340 (Gjachev, 1981). The cylindroidal surface of the cultural mouldboard is formed by a flat guiding  
341 curve, which is a parabola and which is located in a vertical plane, perpendicular to the ploughshare  
342 blade, at a distance of  $2/3$  from its origin. It is defined by two points  $O$  and  $Q$ , and tangents in  
343 them, drawn at angles  $\varepsilon_1$  and  $\varepsilon_2$  to axis  $x$  (Fig. 4, a). Point  $O$  will be located at the origin of the  
344 coordinates, then the coordinates of the second point  $Q$  will be:  $x = L$ ;  $z = H$ . Height  $H$  is  
345 assumed to be equal to 55 cm, but offset  $L$ , angles  $\varepsilon_1$  and  $\varepsilon_2$  can vary within the preset  
346 boundaries. By means of the preset flat guiding curve it is possible to construct a surface of the  
347 mouldboard both of a cylindrical and a cylindroidal shape. If the surface is cylindrical, then all its  
348 rectilinear generatrices are parallel to each other, parallel to the furrow bottom forming angle  
349  $\gamma = 42^\circ$  with the furrow wall. If the surface is cylindrical, then all its rectilinear generatrices are  
350 also parallel to the bottom of the furrow, but with the furrow wall they form a variable angle  $\gamma$   
351 depending on height  $h$  from the bottom of the furrow. Prof. N.Shchuchkin gives graphs of variable  
352 angles  $\gamma = \gamma(h)$ , which he has built as a result of a massive study of the best cultural mouldboards

353 and experimental plough bodies (Shchuchkin, 1982). A graph of this dependence is presented in  
 354 Fig. 4 b, and it can be described by an algebraic curve of the fourth order:

$$355 \quad \gamma = c_1 h^4 + c_2 h^3 + c_3 h^2 + c_4 h + c_5, \quad (27)$$

356 where  $c_1, c_2, c_3, c_4, c_5$  – coefficients found from the condition that the graph is passing through  
 357 characteristic points ( $\gamma = 42^\circ$  at  $h = 0$ ,  $\gamma = 40^\circ$  at  $h = 10$  cm,  $\gamma = 47^\circ$  at  $h = 55$  cm).

358 If the parametric equations of the guiding parabola have the form (Bulgakov, 2011):

$$359 \quad \begin{aligned} x &= (x_Q - 2x_R)v^2 + 2x_R v, \\ h &= (z_Q - 2z_R)v^2 + 2z_R v, \end{aligned} \quad (28)$$

360 where  $v$  – a variable assuming a value within the limits  $v = 0 \dots 1$ ;

361  $x_Q, x_R, z_Q, z_R$  – constant values, found from the preset design parameters  $\varepsilon_1, \varepsilon_2, L, H$ , then

362 the parametric equations of the cylindrical surface of the mouldboard are written as follows:

$$363 \quad \begin{aligned} X &= x \cos \gamma_0 - u \sin \gamma, \\ Y &= x \sin \gamma_0 + u \cos \gamma, \\ Z &= h, \end{aligned} \quad (29)$$

364 where  $u$  – the second independent surface variable specifying the length of the rectilinear  
 365 generatrix;

366  $\gamma = \gamma(h), x = x(v), h = h(v)$  – dependencies presented in (27) and (28);

367  $\gamma_0 = 42^\circ$  – the installation angle of the ploughshare blade to the wall of the furrow.

368

369 If a certain relationship is established between the independent variables  $u$  and  $v$  in the form  $u = u$

370 ( $v$ ), then a line will be assigned on surface (29). Let this line be geodesic for which the dependence

371  $u = u(v)$  will be sought. In this case the equations of the geodesic line are written as follows:

$$372 \quad \begin{aligned} x_g &= x \cos \gamma_0 - u \sin \gamma, \\ y_g &= x \sin \gamma_0 + u \cos \gamma, \\ z_g &= h. \end{aligned} \quad (30)$$

373 In order for the line (30) to be geodesic, equality (3) must be fulfilled:

374

$$\begin{vmatrix} N_x & N_y & N_z \\ x'_g & y'_g & z'_g \\ x''_g & y''_g & z''_g \end{vmatrix} = 0, \quad (31)$$

375 where  $N_x, N_y, N_z$  – coordinates of the unitary vector of the normal to the surface;

376  $x'_g, y'_g, z'_g, x''_g, y''_g, z''_g$  – the first and the second derivatives of equations (30) with respect to the

377 variable  $v$ .

378 Identification of the unitary vector of the normal to the surface is shown in work (Vasilenko, 1980).

379 For the surface (29) we propose a finished result of expressions for the vector along the geodesic

380 line:

381

$$\begin{aligned} N_x &= -z'_g \cos \gamma, \\ N_y &= -z'_g \sin \gamma, \\ N_z &= x'_g \cos(\gamma - \gamma_0) - u\gamma'. \end{aligned} \quad (32)$$

382 The derivatives of equations (30) with respect to variable  $v$  will be:

383

$$\begin{aligned} x'_g &= x' \cos \gamma_0 - u' \sin \gamma - u\gamma' \cos \gamma, \\ y'_g &= x' \sin \gamma_0 + u' \cos \gamma - u\gamma' \sin \gamma, \\ z'_g &= h', \end{aligned} \quad (33)$$

384

$$\begin{aligned} x''_g &= x'' \cos \gamma_0 + (u\gamma'^2 - u'') \sin \gamma - (u\gamma'' + 2u'\gamma') \cos \gamma, \\ y''_g &= x'' \sin \gamma_0 - (u\gamma'^2 - u'') \cos \gamma - (u\gamma'' + 2u'\gamma') \sin \gamma, \\ z''_g &= h''. \end{aligned} \quad (34)$$

385 Since  $\gamma = \gamma(h)$  according to (27), but  $h = h(v)$  according to (28), the first and the second

386 derivatives of angle  $\gamma$  will be written in the following way:

387

$$\gamma' = \frac{d\gamma}{dh} \frac{dh}{dv}, \quad (35)$$

388

$$\gamma'' = \left( \frac{d\gamma}{dh} \frac{dh}{dv} \right)' = \frac{d^2\gamma}{dh^2} \left( \frac{dh}{dv} \right)^2 + \frac{d\gamma}{dh} \frac{d^2h}{dv^2}. \quad (36)$$

389 Substitution of expressions (32) and (33) by (35, 36) into (31) leads to a differential equation of the

390 following form:

$$u'' = \frac{A - B + C + D + E}{F}, \quad (37)$$

where the components that are functions of variable  $v$  have the following expressions:

$$\begin{aligned} A &= \gamma'^2 u (2\gamma'^2 u^2 + 4u'^2 + 2z_g'^2 + x_g'^2) + u' (2\gamma' \gamma'' u^2 + 2z_g' z_g'' + x_g' x_g''), \\ B &= \left[ u x_g' (2\gamma'^3 u + \gamma'' u') + \gamma' u' (2u' x_g' + u x_g'') \right] \cos(\gamma - \gamma_0), \\ C &= x_g' (\gamma'^2 x_g' u + x_g'' u') \cos[2(\gamma - \gamma_0)], \\ D &= 2 \left[ \gamma' u (\gamma' u x_g'' - 2\gamma' u' x_g' - \gamma'' u x_g') + z_g' (x_g'' z_g' - x_g' z_g'') \right] \sin(\gamma - \gamma_0), \\ E &= x_g' (\gamma'' u x' + 2\gamma' u' x_g' - \gamma' u x_g'') \sin[2(\gamma - \gamma_0)], \\ F &= 2\gamma'^2 u^2 + 2z_g'^2 + x_g'^2 - 4\gamma' u x_g' \cos(\gamma - \gamma_0) + x_g'^2 \cos[2(\gamma - \gamma_0)]. \end{aligned} \quad (38)$$

394

### 3. Results and discussion

395 The obtained differential equation (37), taking into account equations (38), was solved by numerical  
 396 methods on the PC. The integration constants were selected in such a way that the geodesic line  
 397 started at a preset point of the blade and crossed it at angle  $\gamma_o = 42^\circ$ , accepted for the ploughs. The  
 398 obtained dependence  $u = u(v)$  was inserted into equations (30), according to which a geodesic line  
 399 was built on the surface of the mouldboard (29). We limited the surface of the mouldboard to the  
 400 frontal contour the automated construction of which was described in detail in (Bulgakov, 2011).  
 401 Unlike a cylindrical surface, the values of angle  $\theta$  for the geodesic lines of the same height  
 402 emerging from different points of the mouldboard differ, yet with a slight divergence (Fig. 5).  
 403 Obviously, this divergence will be the greater, the more the cylindroidal surface will differ from the  
 404 cylindrical surface, i.e., from the way of regularity (27), which establishes the distribution law of  
 405 the rectilinear generatrices by height. If  $\gamma = \gamma_o - const$ , the cylindroidal surface turns into a  
 406 cylindrical one, and the value of angle  $\theta$  for the geodesic lines along the length of the mouldboard  
 407 becomes equal.

408 In Fig. 5 for the accepted angles  $\varepsilon_1 = 30^\circ$ ,  $\varepsilon_2 = 95^\circ$ , there are geodesic lines constructed for  
 409 different values of offset  $L$  with the geodesic lines emerging from three points on the mouldboard.  
 410

411 The numerical values of angle  $\theta$  for each line are indicated by an arrow. Comparing the respective  
412 numerical values of angle  $\theta$  for the geodesic lines with different offset values  $L$ , we can conclude  
413 that this indicator increases when value  $L$  increases.

414 In Fig. 6 for the accepted angles  $\varepsilon_1 = 30^\circ$ ,  $\varepsilon_2 = 95^\circ$ , offset  $L = 30$  cm geodesic lines from the  
415 middle point of the blade have been constructed at different arrival angles of the layer arrival onto  
416 the mouldboard, the geodesic line for the accepted value  $\gamma_o = 42^\circ$  being presented by a dashed line.

417  
418 At the arrival angles close to  $90^\circ$ , the value of angle  $\theta$  is the largest, and the arrival angle  
419 decreasing, it also decreases, but not so as on a cylindrical surface where this regularity is described  
420 analytically.

421 Let us find out how angle  $\theta$  depends on angles  $\varepsilon_1$  and  $\varepsilon_2$  (Fig. 4 a) for the corresponding shape of  
422 the guiding curve. Fig. 7 a presents three mouldboards with different offsets and geodesic lines  
423 emerging from the middle of the blade, depicted so that the blade is projected into a point.

424 Apparently, increase in value  $\theta$  is due to the increase in the path of the layer when it is raised to  
425 the same degree. In Fig. 7 b geodesic lines from the middle point of the blade are constructed by  
426 numerical integration, indicating angle  $\theta$  for different values of angles  $\varepsilon_1$  and the accepted values

427  $L = 30$  cm,  $\varepsilon_2 = 95^\circ$ , and in Fig. 7 c – for different values of angles  $\varepsilon_2$  and the accepted values  $L$   
428  $= 30$  cm,  $\varepsilon_1 = 30^\circ$ . It is evident from the obtained results that, angle  $\varepsilon_1$  increasing, the value of  
429 angle  $\theta$  decreases, but, when angle  $\varepsilon_2$  increases, on the contrary, it also increases.

430

#### 431 **4. Conclusions**

432 1. The dynamic component of the draught resistance of the plough, the value of which is directly  
433 proportional to the square of the ploughing velocity, can be estimated by the value of a  
434 dimensionless coefficient, conditionally named the wrapping angle of the layer. This parameter  
435 for the mouldboard surface can be found if the path of the movement of the mid-point of the  
436 layer section is known. If the geodesic line is taken as the curve of the layer movement as a

437 limiting path, the problem is reduced to finding the corresponding value of the wrapping angle.

438 2. For cylindrical surfaces, the geodesic line intersects all the generatrices at a constant angle, and  
439 the wrapping angle depends on the value of this angle and the length of the line on the  
440 mouldboard.

441 3. For cylindroidal surfaces, the angle of the section is variable; therefore it is not possible to  
442 establish certain analytical regularities to determine the geodesic lines with the predicted value of  
443 the wrapping angle. However, by numerical methods it is possible to determine the impact of one  
444 or another design parameter of the mouldboard upon the value of the wrapping angle of the  
445 layer, which is directly related to the value of the dynamic component of the draught resistance.

446 4. The proposed approach is not the determining (most important) for designing mouldboards, since  
447 it takes into account only the geometry of the surface without considering other agrotechnical  
448 requirements. For instance, the dynamic component of the resistance will completely disappear if  
449 the surface turns into a flat wedge; yet in this case no turn of the layer will take place. Therefore,  
450 a search for the ways how to reduce the wrapping angle of the layer carried out by mouldboard  
451 should be combined with the quality requirements of ploughing.

452

### 453 **Acknowledgements**

454

455 This research did not receive any specific grant from funding agencies in the public, commercial, or  
456 not-for-profit sectors. The Authors equally contributed to the present study.

457

### 458 **References**

459

460 Abo-Elnor, M., Hamilton, R., Boyle, J., 2004. Simulation of soil-blade interaction for sandy soil  
461 using advanced 3D finite element analysis. *Soil Tillage Res.* 75, 61–73.

462

463 Bentaher, H., Ibrahmi, A., Hamza, E., Hbaieb, M., Kantchev, G., Maalej, A., Arnold, W., 2013.  
464 Finite element simulation of moldboard-soil interaction. *Soil Tillage Res.* 134, 11–16.  
465

466 Bentaher, H., Hamza, E., Kantchev, G., Maalej, A., Arnold, W., 2008. Three-point hitch-  
467 mechanism instrumentation for tillage power optimization. *Biosystems Engineering* 100, 24–30.  
468

469 Bulgakov, V. 2010. Designing a plough mouldboard for a prescribed geodesic line - the limiting  
470 path of movement. In: *Scientific Herald of the National University of Life and Environmental*  
471 *Sciences of Ukraine*, 144 (5), 20-35.  
472

473 Bulgakov, V. 2011. Automated construction of a 3D model of a plough mouldboard with a  
474 cylindriodal surface. In: *Scientific Herald of the National University of Life and Environmental*  
475 *Sciences of Ukraine*, 166 (2), 51-62.  
476

477 Chi, L., Kushwaha, R., 1990. A non-linear 3-D finite element analysis of soil failure with tillage  
478 tools. *J. Terramech.* 27, 343–366.  
479

480 Gjachev, L. 1981. A theory of the ploughshare-mouldboard surface. *Science, Zernograd*  
481

482 Goryachkin, V. 1998. *Collected works in three volumes. Vol.1. Kolos, Moskow.*  
483

484 Karmakar, S., Kushwaha, R.L., 2006. Dynamic modeling of soil–tool interaction: an overview from  
485 a fluid flow perspective. *Journal of Terramechanics* 43, 411–425  
486

487 Shmulevich, I., 2010. State of the art modeling of soil-tillage interaction using discrete element  
488 method. *Soil Tillage Res.* 111, 41–53.  
489



490 Tong, J., Moayad, B.Z., 2006. Effects of rake angle of chisel plough on soil cutting factors and  
491 power requirements: a computer simulation. *Soil & Tillage Research* 88, 55–64  
492

493 Rucins, A., Vilde, A.J., Nowak, J. 2007. Impact of the share inclination angle on the ploughing  
494 resistance. In: TEKA Commission of Motorization and Power Industry in Agriculture, VII, 199-  
495 209. Polish Academy of Sciences Branch in Lublin, Lublin, Poland  
496

497 Shchuchkin, N. 1982. *Ploughs and shallow ploughs*. Mechanical engineering, Moskow.  
498

499 Vasilenko, P. 1980. A theory of the movement of a particle across rough surfaces of agricultural  
500 machines. Kiev.  
501

502 Vilde, A. 2012. Profilograms of share-mouldboards surfaces of some typical plough bodies. In:  
503 Proceedings of 11th International Scientific Conference “Engineering for Rural Development”,  
504 Jelgava, 11, 81-87.  
505

506 Vilde, A., Rucins, A. 2008. Simulation of the impact of the plough body parameters, soil properties  
507 and working modes on the ploughing resistance. In: Proceedings - UKSim 10th International  
508 Conference on Computer Modelling and Simulation, EUROSIM/UKSim2008, Cambridge; United  
509 Kingdom, 697-702.  
510

511 Vilde, A. 2004 Mechanical and mathematical foundations for modelling the dynamics of soil tillage  
512 machine operating parts. In: TEKA Commission of Motorization and Power Industry in Agriculture,  
513 4, 228-236. Polish Academy of Sciences Branch in Lublin. Lublin, Poland  
514

515 Volkov, Y. 2002. “Geodesic line”. In: Hazewinkel Michiel , Enciklopedia of Matematics,, Springer  
516 Science+Business Media B.V. / Kluwer Academic Publishers, ISBN 978-1-55608-010-4.

517

518 Zhang, L.B., Cai, Z.X., Liu, H.F., 2018. A novel approach for simulation of soil-tool interaction  
519 based on an arbitrary Lagrangian–Eulerian description. Soil and Tillage Research, 178, 41-49.

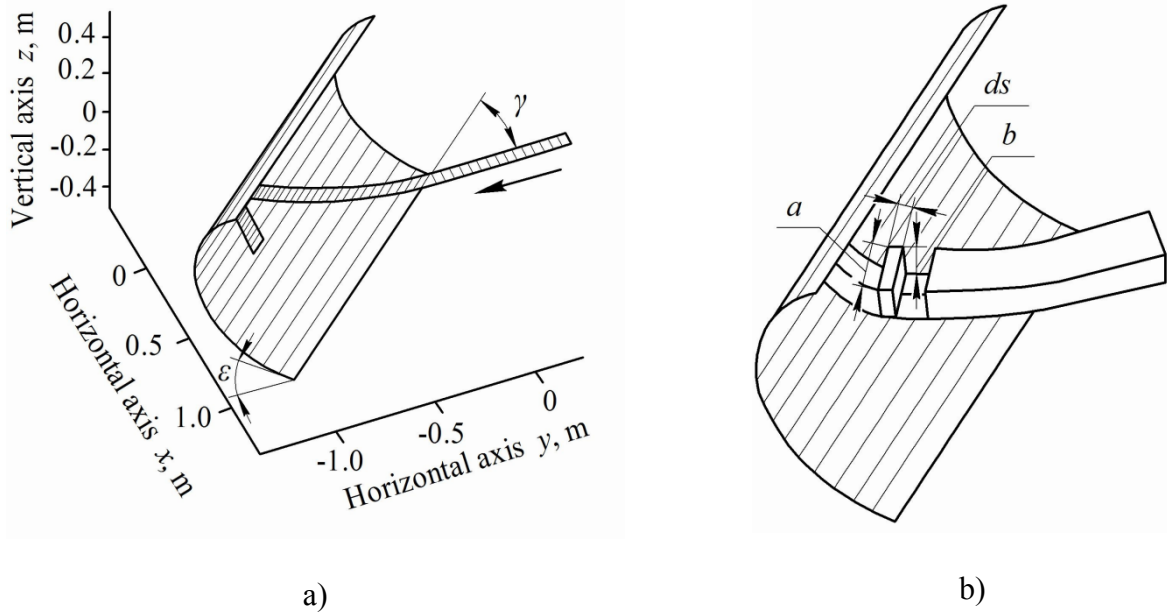
520

521 Zhu, L., Ge, J.-R., Cheng, X., Peng, S.-S., Qi, Y.-Y., Zhang, S.-W., Zhu, D.-Q., 2017. Modeling of  
522 share/soil interaction of a horizontally reversible plow using computational fluid dynamics. J.

523 Terramech. 72, 1–8.

524

525



528

529 Fig. 1. On determination of the direction of movement of the soil layer along the cylindrical surface:

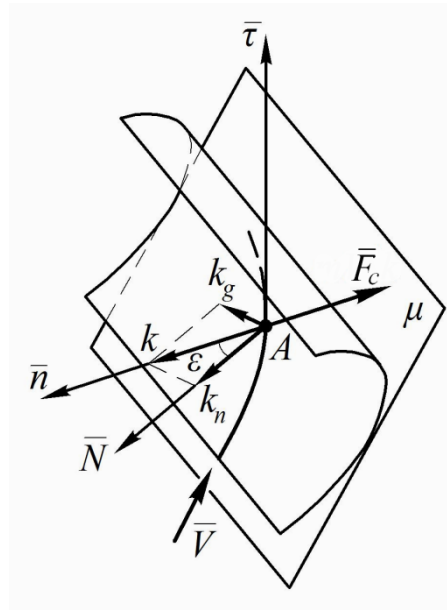
530 a) simulation of the movement of the layer along the inner surface by means of a flexible elastic

531 band that crosses all generating surfaces at a constant angle  $\gamma$  ; b) geometric dimensions of the layer

532 and its infinitesimal element in the form of a parallelepiped

533

535



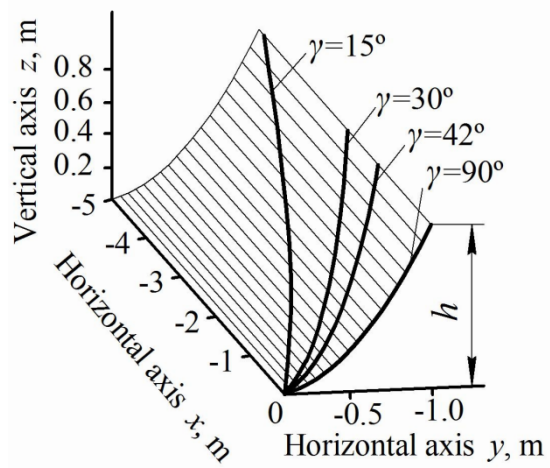
536

537

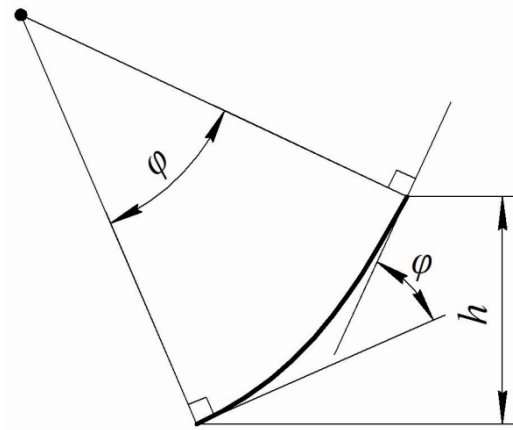
538 Fig. 2. Decomposition of the curvature vector and the forces acting upon the element of the layer at

539 point  $A$  of the path of its movement at velocity  $V$

540



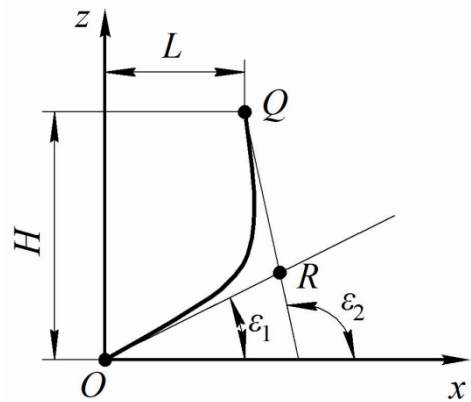
a)



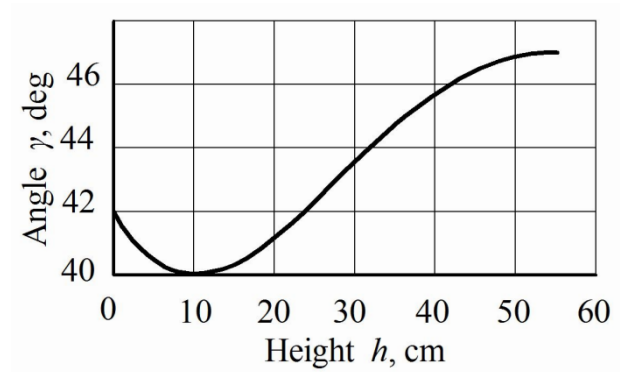
b)

543

544 Fig. 3. A cylindrical surface defined by expression (22), and its projection onto a plane,  
 545 perpendicular to the rectilinear generatrices: a) geodesic lines on the surface indicating the value of  
 546 angle  $\gamma$  ; b) an orthogonal section of the surface with tangents and normals at the ends of the curve

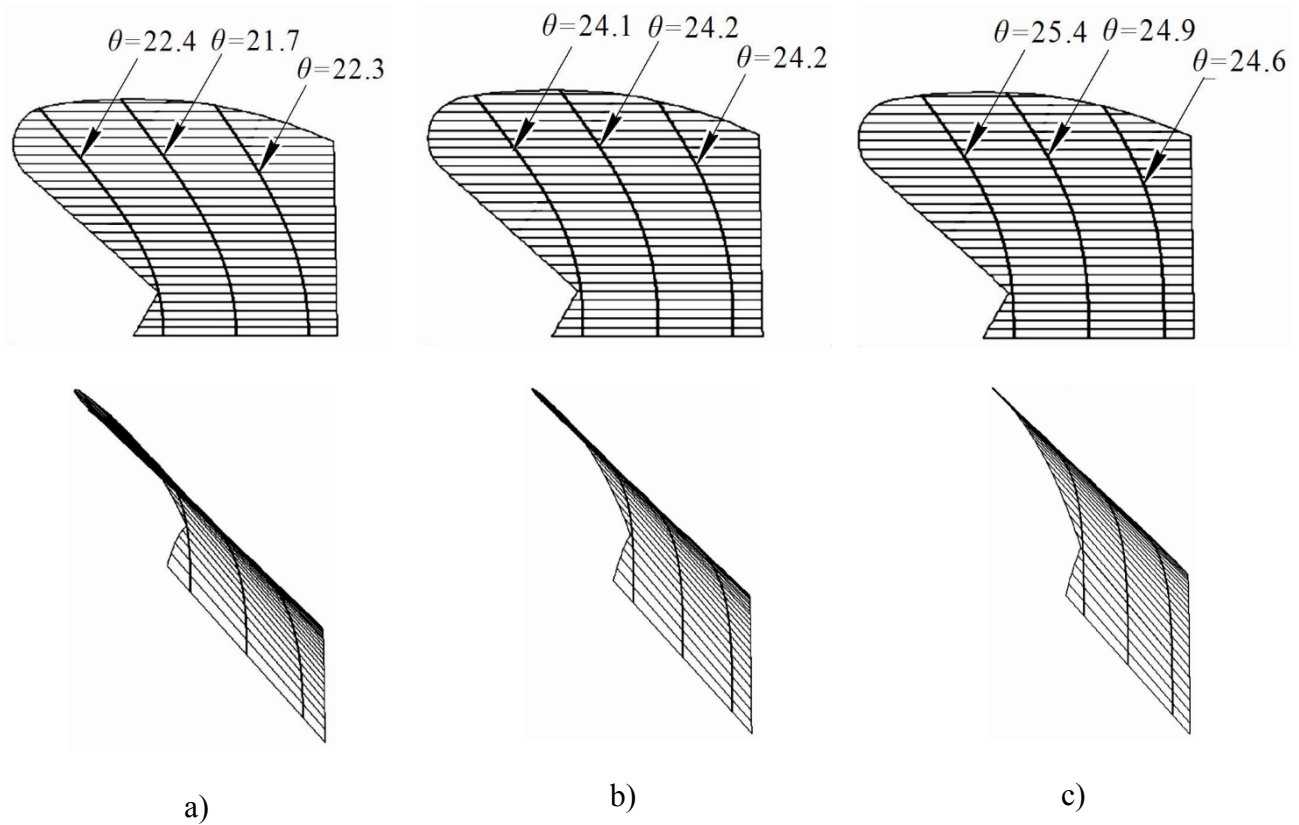


a)



b)

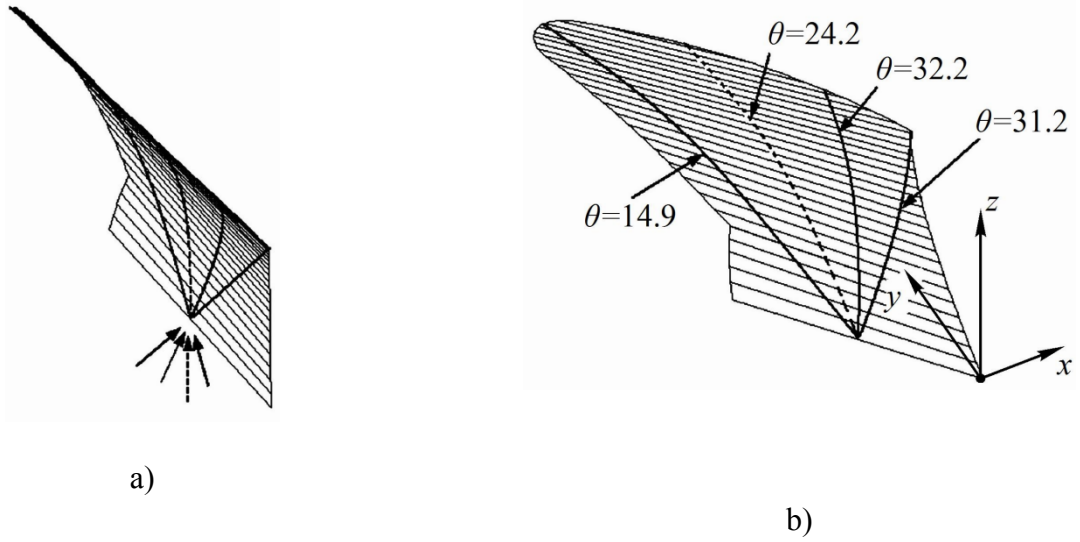
549 Fig. 4. On the definition of a particular surface of a cultural mouldboard: a) the guiding curve (the  
 550 parabola in a vertical plane, perpendicular to the ploughshare); b) a graph of the variable inclination  
 551 angle  $\gamma = \gamma(h)$  of the rectilinear surface generatrix to the furrow wall



554

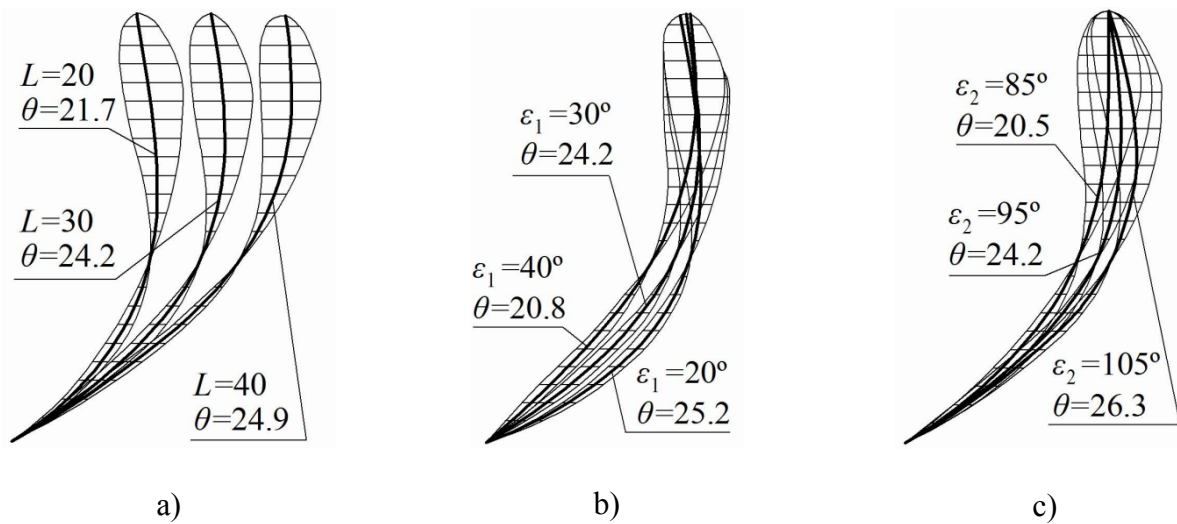
555 Fig. 5. Cultural mouldboards of ploughs (in two projections) with geodesic lines for the preset  
 556 design parameters  $\varepsilon_1 = 30^\circ$ ,  $\varepsilon_2 = 95^\circ$  and various offset values (see Fig. 4 a): a)  $L = 20$  cm; b)  $L$   
 557  $= 30$  cm; c)  $L = 40$  cm

558



561 Fig. 6. a) Direction of arrival of the soil layer; b) the value of the wrapping angle of the  
562 corresponding path for a cultural mouldboard





566

567 Fig. 7. Geodesic lines emerging from the middle of the blade, and corresponding values of angle  $\theta$   
 568 for various forms of the guiding parabola of a cultural (cylindroidal) mouldboard: a) a different  
 569 offset value  $L$  for the accepted angles  $\varepsilon_1 = 30^\circ$ ,  $\varepsilon_2 = 95^\circ$ ; b) a different value of angle  $\varepsilon_1$  at the  
 570 accepted values  $\varepsilon_2 = 95^\circ$ ,  $L = 30$  cm; c) a different value of angle  $\varepsilon_2$  at the accepted values  $\varepsilon_1$   
 571  $= 30^\circ$ ,  $L = 30$  cm

572